RESEARCH HIGHLIGHT

Supersensitive odor discrimination is controlled in part by initial transient interactions between the most sensitive dorsal olfactory receptors and G-proteins

Takaaki Sato[1], Reiko Kobayakawa[2], Ko Kobayakawa[2], Makoto Emura[3], Shigeyoshi Itohara[4], Takashi Kawasaki[1], Akio Tsuboi[5], Hiroyoshi Matsumura[6]

[1]*Biomedical Research Institute, National Institute of Advanced Industrial Science and Technology, Amagasaki, Hyogo 661-0974, Japan*
[2]*Institute of Biomedical Science, Kansai Medical University, Hirakata, Osaka 573-1010, Japan*
[3]*Takasago International Corporation, Hiratsuka, Kanagawa 254-0073, Japan*
[4]*Laboratory for Behavioral Genetics, Brain Science Institute, RIKEN, Wako, Saitama 351-0198, Japan*
[5]*Research Institute of Frontier Medicine, Nara Medical University, Kashihara, Nara 634-8521, Japan*
[6]*Department of Applied Chemistry, Graduate School of Engineering, Osaka University, Suita, Osaka 565-8571, Japan*

Correspondence: Takaaki Sato
E-mail: taka-sato@aist.go.jp
Received: November 11, 2015
Published online: January 15, 2016

Pairs of enantiomeric odor ligands are difficult to resolve by instrumental analyses because compounds with mirror-image molecular structures have almost identical physicochemical properties. The olfactory system, however, discriminates (–)-forms of enantiomers from their (+)-forms within seconds. To investigate key olfactory receptors for enantiomer discrimination, we compared behavioral detection and discrimination thresholds of wild-type mice with those of ΔD mice that lack all dorsal olfactory receptors. Surprisingly, wild-type mice displayed an exquisite "supersensitivity" to enantiomeric pairs of wine lactones and carvones in both detection and discrimination tasks using odor plume-like flows in a Y-maze. In contrast, ΔD mice showed $>10^{10}$-fold reductions in enantiomer discrimination sensitivity compared to wild-type mice. ΔD mice detected one or both of the (–)- and (+)-enantiomers over a wide concentration range, but were unable to discriminate them. This "enantiomer odor discrimination paradox" indicates that the most sensitive dorsal receptors play a critical role in hierarchical odor coding for enantiomer identification. In addition, to identify residues responsible for the rapid and robust response of murine olfactory receptor S6 (*mOR-S6*) via chimeric $G\alpha_{15\_olf}$, mutations of the C-terminal helix 8 were analyzed in a heterologous functional expression system. The N-terminal hydrophobic core between helix 8 and TM1−2 of *mOR-S6* is important for Gα activation. A point mutation of a helix 8 N-terminal acidic residue eliminated the improved response dynamics via the chimeric $G\alpha_{15\_olf}$. This result suggests that an N-terminal acidic residue of helix 8 is responsible for rapid Gα activation. Supersensitive odor discrimination is thus largely governed by signals from the most sensitive dorsal olfactory receptors with the shortest onset latencies, which are controlled in part by initial transient interactions between the receptor C-terminal helix 8 and the Gα C-terminal region.

Keywords: G-protein-coupled receptor; olfactory receptor; mouse; human; odor coding; initial interaction

The olfactory system discriminates enantiomers sensitively and rapidly within seconds. The olfactory information processing is initiated by stereospecific ligand binding to olfactory receptors (ORs) and allows the perception of the odor identity of a given ligand. ORs are members of the G-protein-coupled receptor (GPCR) superfamily, which includes visual receptors and neurotransmitter receptors. The number of OR family members is more than 100-fold greater than that of visual receptors. In mice and humans, each olfactory sensory neuron (OSN) expresses one of approximately 1,000 and 350 different types of ORs [1-4], respectively, that operate as independent coding channels. The sensory profile of an odor stimulus may include several distinct elemental odors if multidimensional input is segmented through parallel pathways [5]. It is likely that, analogous to the process by which the color orange is hierarchically decoded as yellowish red or reddish yellow by signals from three types of the visual receptors, elemental odors are decoded by multiple receptors hierarchically through a temporal coding scheme that prioritizes the most sensitive, best-tuned receptors [6-8]. These receptors would dominate the perceived odor qualities by relaying the earliest ascending signals to cortical targets, evoking specific elemental odors, and recruiting feedforward inhibition to suppress competing odors evoked by longer latency OR inputs that are initially weaker and become stronger at later times. We previously estimated that enantiomers of carvone (at 100 μM) activated 70 types of murine ORs with >80% overlap [6]. The high overlap at higher odorant concentrations suggested that a minority of the most sensitive receptors plays a key role in determining odor quality differences between enantiomers and enabling their discrimination. Our hierarchical odor coding model predicts selective shifts in perceived odors by mutual inhibition when different stimuli are mixed [8]. For example, 2,5-dihydro-2,4,5-trimethylthiazoline (TMT) induces stress responses in mice when recognized as a predator odor [9]. The stress responses are reduced in different ways through feedforward inhibition when TMT is mixed with rose or hinokitiol odors, but not with (S)-(+)-carvone [10, 11]. These led us to formulate a model of odor quality coding in which signals transduced by cognate receptors and relayed as inputs through segregated channels in the olfactory bulb [12-14] are processed in the olfactory cortex to evoke "elemental" perceived odor qualities by feedforward, feedback, and associative connections [6-8, 15-18].

Recently, we discovered a "supersensitivity" of wild-type (WT) mice to sub-ppq (<10^{-15}) level enantiomeric pairs of wine lactones and carvones in both detection and discrimination tasks in a Y maze (Figure 1A) [8]. This supersensitivity may be surprising given that these compounds are usually regarded as general odorants. Extreme sensitivity is often associated with innate responses to semiochemicals such as allomones and pheromones [19]. We previously showed that ΔD mice, which lack all dorsal olfactory receptors, are able to detect an allomone of rodent predators, TMT, but cannot recognize it as a predator odor [9]. The reported thresholds of WT and ΔD mice for TMT were equally low at 1.3×10^{-8} w/w, and much lower than for 2-methylbutyric acid (5.7×10^{-5} and 5.7×10^{-4} w/w, respectively) in the habituation-dishabituation test [8, 9]. Instead of TMT, we used non-dihydrogenated TMT (nTMT) to avoid potential problems arising from exposing WT mice to >2 weeks of repeated assays with the innate stressor TMT. We observed supersensitive detection of nTMT in both WT mice (10^{-21} w/w) and ΔD mice (10^{-19} w/w) (Figure 1A) [8]. These findings were archived by employing negative pressure-guided odor plume-like flows in the Y-maze with modified experimental procedures. Moths and other insects supersensitively navigate their way to scent sources along odor plumes [20, 21]. The Y-maze design was optimized to direct plumes of odorized air along the central axis of each maze arm, maintaining radial concentration gradients between the central axis and arm walls.

Dorsal receptors may play special roles in odor coding and recognition. As expected, our approach revealed an "enantiomer odor discrimination paradox" in ΔD mice that showed >10^{10}-fold reductions in enantiomer discrimination sensitivity compared to wild-type mice [8]. ΔD mice were able to detect, but not discriminate one or both of the (–)- and (+)-enantiomers over a wide concentration range. This result strongly supports our hypothesis of hierarchical odor coding at least for enantiomer identification [8] and likely for fine odor discrimination between genetically determined body odors and their disease-induced alterations [22-24]. Notably, ΔD mice showed selective major loss of sensitivity to the (+)-enantiomers. The resulting 10^{8}-fold differential sensitivity of ΔD mice to (–)- vs. (+)-wine lactone matched that observed in humans (Figures 1A, 1B) [8, 25]. This suggests that humans lack highly sensitive orthologous dorsal receptors for the (+)-enantiomer, similarly to ΔD mice. Elemental odors encoded by subsets of orthologous ORs may be broadly conserved across species. Patterns of similarity among murine OR codes for 12 odorants resembled groupings of human percepts of the same odorant set [26]. Notably, three distinct subsets of murine ORs completely
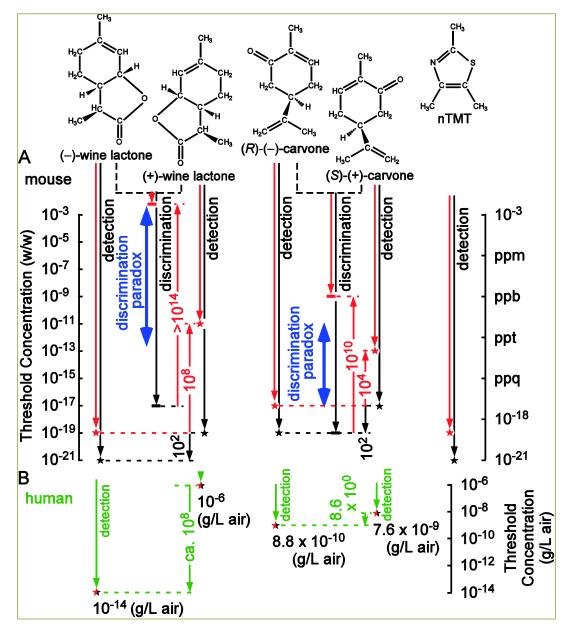
Figure 1. Odor detection and discrimination thresholds for wine lactone and carvone enantiomer pairs in WT mice, ΔD mice and human. A, Plots of detection and discrimination range (arrows) and threshold (asterisks) for enantiomer pairs of odorants in WT mice (black plots) and ΔD mice (red plots) in the Y-maze. Odorant threshold concentrations (w/w); 10^{-17}-10^{-21} w/w (10^{-2}-10^{-6} ppq) for WT mice, 10^{-11}-10^{-19} w/w (10^{1} ppt-10^{-4} ppq) for ΔD mice. For wine lactones, the sensitivity difference between enantiomers was similar in humans and ΔD mice (10^{8}-fold, green and red arrows between broken lines, respectively). However, for carvones, the differences in WT and ΔD mouse strains, and humans, were inconsistent (10^{2}-, 10^{4}-, and 8.6-fold, black, red, and green arrows, respectively). Despite retention of high detection sensitivity to (−)-enantiomers, ΔD mice showed a >10^{10}-fold reduction in discrimination sensitivity. This leads to an enantiomer odor discrimination paradox, in which ΔD mice detected one or both of the (−)- and (+)-enantiomers but could not discriminate them over a wide concentration range (blue arrows). **B**, Detection thresholds in humans (black-red asterisks) as reported previously [25, 27]. The differences in odorant detection thresholds are about 10^{8}- and 8.6-fold for wine lactone and carvone enantiomers, respectively. Reprint with permission for authors [8].

matched human odor percepts of vanilla, creamy, and cinnamon. The human olfactory system detects (−)- and (+)-enantiomers of carvones with nearly equal sensitivity [27]. Moreover, humans are roughly 10^{5}-fold less sensitive to

(R)-(−)-carvone than to (−)-wine lactone. The observed 10^{4}-fold differences in sensitivities of ΔD mice were much greater than the corresponding sensitivity difference in humans (Figure 1) [8]. These results indicate that humans

express neither the orthologous murine ORs most sensitive to (*S*)-(+)-carvone, nor the dorsal and ventral ORs most sensitive to (*R*)-(−)-carvone. Humans express fewer than half the number of ORs found in mice. Absence of the most sensitive orthologous ORs likely accounts for the much poorer detection and discrimination performance of humans compared to mice.

The basic concept of hierarchical odor coding is that the earliest arriving signals from the most sensitive, short latency, cognate receptors are the first to activate inhibitory feedforward pathways in the olfactory cortex through short-latency olfactory bulb tufted cells [8]. These early inhibitory signals from the ventro-rostral part of the anterior piriform cortex [15], receiving signals from a minority of the most sensitive receptors, will trigger synchrony of cognate receptor signal inputs to pyramidal cells that selectively evoke "elemental" odor percepts by engaging associative neural pathways. The processing cascade may also suppress other odors corresponding to less sensitive, long latency, non-cognate ORs. The model hypothesizes that unique elemental odors correspond to a relatively small set of narrowly tuned ORs with highest sensitivities to a target ligand, whereas common elemental odors correspond to more broadly tuned ORs with overlapped sensitivity to multiple ligands. Primary qualities of odor percepts are determined by unique elemental odors and are modulated by secondary qualities from common odors.

To understand the origins of striking sensitivity differences between enantiomers of wine lactones and carvones, we compared dose-dependent changes in receptor codes. Using Ca^{2+} imaging to profile odorant responses of OSNs of WT mice, we found that OR coding was sparser for wine lactones than carvones, i.e. wine lactone-sensitive ORs were about three-fold less numerous than carvone-sensitive ORs [8]. Sparse coding is consistent with the greater impact of dorsal OR ablation on behavioral detection thresholds of wine lactones. The largest subpopulations of the most sensitive ORs were those best-tuned to (−)-wine lactone or those with overlapping sensitivity to (−)-/(+)-wine lactones. These proportions held at all tested concentrations, except for (+)-wine lactone at 1 µM [8]. Moreover, we did not observe (+)-wine lactone-sensitive ORs, except for one OR at concentrations <100 µM [8]. These data are consistent with sparse coding of (+)-wine lactone by a small set of the most sensitive and specific dorsal ORs.

In contrast, (*R*)-(−)- and (*S*)-(+)-carvones are represented peripherally by different classes of the most-sensitive, best-tuned murine ORs: i.e., (*R*)-(−)-carvone-best ORs for the odor of (*R*)-(−)-carvone vs. a combination of (*S*)-(+)-carvone-best ORs and (*R*)-(−)-/(*S*)-(+)-carvone-best
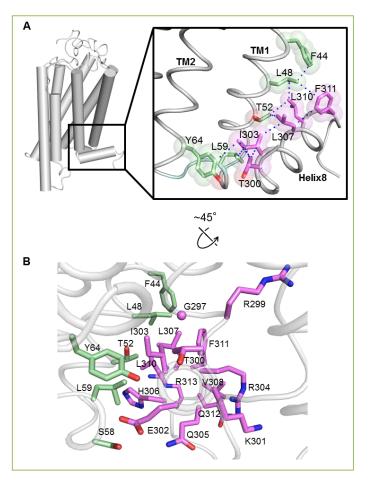

Figure 2. Model of mOR-S6 generated by homology modeling. **A**, A whole model of *mOR-S6* (left). The right figure represents enlarged views around the helix 8, which are crucial for the experimental design. The residues in hydrophobic interactions surrounding helix 8 are shown as transparent CPK spheres and labeled. The residues of helix 8 are magenta, while TM1 and TM2 residues are green. **B**, The detailed interfaces of helix 8 and TM1−2, rotated 45° from the top panels. The residues in hydrophobic interactions surrounding helix 8 are shown as stick models. Reprint with permission for authors [32].

(overlapping, equally sensitive) ORs for the odor of (*S*)-(+)-carvone [6, 8]. According to our model, the difference in populations of the most sensitive receptors would translate into different perceived elemental odors, enabling WT mice to discriminate between (*R*)-(−)- and (*S*)-(+)-carvones even at the very low detection threshold concentration of 10^{-19} w/w (Figure 1**A**). We illustrated specific enantiomer-dependent temporal orders (latencies) of receptor input to the olfactory pathway as predicted by our model, for 15 identified carvone-responsive ORs (see Figs. 3J, 3K in reference 8). Temporal ordering of activation was inferred from indirect measurements, not actual latency times, i.e., relative response amplitudes of ORs in a heterologous functional expression system [28] or isolated OSNs [6] (Supplementary Information Table ST3 in reference 8). For example, slightly greater response amplitudes of *mORcar-n270* and *mORcar-n266* to

(R)-(–)- and (S)-(+)-carvones, respectively, were depicted by slight left shifts of the positions of their signal bars compared to those of other enantiomers [8]. Therefore, this prediction of signal ordering is approximate, and may be modified by other determinants of input latency [29, 30]. By using the 15 identified carvone ORs, our model explained how a deletion of just one most sensitive dorsal OR (*mORcar-c5*) could significantly alter early OR signaling for (R)-(–)-carvone to those of (R)-(–)-/(S)-(+)-carvone-best (overlapping, equally sensitive) ORs that would code common elemental odors as the principal elemental odors of (R)-(–)-carvone in ΔD mice [8].

The large reduction in the detection sensitivity to (S)-(+)-carvone in ΔD mice may be explained by a loss of most of the most sensitive (S)-(+)-carvone-best ORs. In the absence of highly sensitive (S)-(+)-carvone-best ORs, weak subthreshold signals from common ORs may fall below the detection threshold for pyramidal cells of the olfactory cortex, and prevent ΔD mice from perceiving any difference between (R)-(–)- and (S)-(+)-carvones. In our model, the simplest interpretation is that signals of the most sensitive (R)-(–)-/(S)-(+)-carvone-best ORs dominate the principal elemental odors for both (R)-(–)- and (S)-(+)-carvones with no emphasis on a weak but unique elemental odor, so that ΔD mice only perceive a common (R)-(–)-/(S)-(+)-carvone odor and fail to discriminate the enantiomers [8]. In insects, fine discrimination of similar odorants is impaired by desynchronization of antennal lobe output neurons by picrotoxin, which blocks $GABA_A$ receptor-mediated synchrony [31]. In mammals, such inhibitory signal-mediated synchronization of olfactory bulb mitral/tufted cells could serve to bind signals from selected subsets of cognate (or other) ORs for downstream readout by coincidence detection in cortical pyramidal cells of the anterior piriform cortex. At present, the precise synaptic and network mechanisms in the olfactory bulb and cortex that could underlie hierarchical odor coding remain to be elucidated, besides OR-dependent differences in response onset latencies.

In the heterologous functional expression system, response onset latencies of ORs were shortened by using a chimeric $G\alpha_{15\_olf}$ that possessed the C-terminal tail of the $G\alpha_{olf}$ [28]. This means that mutations of the interactive sites of the most sensitive dorsal ORs to $G\alpha_{15\_olf}$ may change temporal ordering of OR input to the brain as well as hierarchical odor coding. To identify residues responsible for rapid and robust response of murine olfactory receptor S6 (*mOR-S6*) via the chimeric $G\alpha_{15\_olf}$, mutations of the C-terminal helix 8 were analyzed in the functional expression system. The N-terminal hydrophobic core between helix 8 and TM1−2 of *mOR-S6* is important for Gα activation (Figure 2) [32]. A point mutation of a helix 8 N-terminal acidic residue eliminated the improved response dynamics via the chimeric $G\alpha_{15\_olf}$ [32]. Atomic resolution structures of GPCR complexes with G proteins were reported for rhodopsin and β_2 adrenergic receptor [33-36]. GPCRs stably interact with G proteins through their intracellular domains including the DRY motif in the transmembrane domain 3 (TM3). Significant residues controlling receptor−G-protein coupling are believed to be generally located at the intracellular end of TM5, the N-terminal region of intracellular loop 3 (IL3), the junction of TM3 and IL2, the C-terminal TM6, and the junction of TM7 and helix 8 [37]. In many GPCRs, an amphipathic helix 8 in the C-terminal domain plays several key roles in protein/lipid interaction [38, 39], receptor internalization [40], dimerization of receptors [41], and coupling with G proteins [42, 43]. Understanding intra- and intermolecular interactions in GPCRs and conformational changes between intramembrane and cytoplasmic domains are crucial for elucidation of GPCR activation mechanisms. It was reported that helix 8 interacted with the NPxxY motif in TM7, highly conserved residues in GPCRs [34, 44, 45]. Mutation within this motif caused a significant reduction in signal activity [45, 46]. It was also shown that a proximal dibasic motif in helix 8 was important for GPCR signaling [47]. These results suggest that an N-terminal acidic residue of helix 8 is responsible for rapid Gα activation via initial transient interaction. The supersensitive odor discrimination is largely governed by signals from the most sensitive dorsal olfactory receptors with the shortest onset latencies, which are controlled in part by initial transient interactions between the C-terminal helix 8 of receptors and the C-terminal region of Gα.

Conflicting interests

The authors have declared that no competing interests exist.

Acknowledgements

Present address

Hiroyoshi Matsumura: College of Life Sciences, Ritsumeikan University, Kusatsu, Shiga 525-8577, Japan

References

1. Buck L, Axel R. A novel multigene family may encode odorant receptors: a molecular basis for odor recognition. Cell 1991; 65:175-187.

2. Zhang X, Firestein S. The olfactory receptor gene superfamily of the mouse. Nat Neurosci 2002; 5:124-133.

3. Malnic B, Hirono J, Sato T, Buck L. Combinatorial receptor codes for odors. Cell 1999; 96:713-723.

4. Serizawa S, Miyamichi K, Sakano H. One neuron-one receptor rule in the mouse olfactory system. Trends Genet 2004; 20:648-653.

5. Rokin D, Hemmelder V, Kapoor V, Murthy VN. An olfactory cocktail party: figure-ground segregation of odorants in rodents. Nat Neurosci 2014; 17:1225-1232.

6. Hamana H, Hirono J, Kizumi M, Sato T. Sensitivity-dependent hierarchical receptor codes for odors. Chem Senses 2003; 28:87-104.

7. Sato T, Hirono J, Hamana H, Ishikawa T, Shimizu A, Takashima I, *et al*. Architecture of odor information processing in the olfactory system. Anat Sci Int 2008; 83:195-206.

8. Sato T, Kobayakawa R, Kobayakawa K, Emura M, Itohara S, Kizumi M, *et al*. Supersensitive detection and discrimination of enantiomers by dorsal olfactory receptors: evidence for hierarchical odour coding. Sci Rep 2015; 5:14073.

9. Kobayakawa K, Kobayakawa R, Matsumoto H, Oka Y, Imai T, Ikawa M, *et al*. Innate versus learned odour processing in the mouse olfactory bulb. Nature 2007; 450:503-508.

10. Matsukawa M, Imada M, Murakami T, Aizawa S, Sato T. Rose odor can innately counteract predator odor. Brain Res 2011; 1381:117-123.

11. Murakami T, Matsukawa M, Katsuyama N, Imada M, Aizawa S, Sato T. Stress-related activities induced by predator odor may become indistinguishable by hinokitiol odor. Neuroreport 2012; 23:1071-1076.

12. Mombaerts P, Wang F, Dulac C, Chao SK, Nemes A, Mendelsohn M, *et al*. Visualizing an olfactory sensory map. Cell 1996; 87:675-686.

13. Wang F, Nemes A, Mendelsohn M, Axel R. Odorant receptors govern the formation of a precise topographic map. Cell 1998; 93:47-60.

14. Serizawa S, Miyamichi K, Takeuchi H, Yamagishi Y, Suzuki M, Sakano H. A neuronal identity code for the odorant receptor-specific and activity-dependent axon sorting. Cell 2006; 127:1057-1069.

15. Ishikawa T, Sato T, Shimizu A, Tsutsui K, de Curtis M, Iijima T. Odor-driven activity in the olfactory cortex of an in vitro isolated guinea pig whole brain with olfactory epithelium. J Neurophysiol 2007; 97:670-679.

16. Igarashi KM, Ieki N, An M, Yamaguchi Y, Nagayama S, Kobayakawa K, *et al*. Parallel mitral and tufted cell pathways route distinct odor information to different targets in the olfactory cortex. J Neurosci 2012; 32:7870-7885.

17. Haberly LB. Parallel-distributed processing in olfactory cortex: new insights from morphological and physiological analysis of neuronal circuitry. Chem Senses 2001; 26:551-576.

18. Shipley MT, McLean JH, Ennis M. Olfactory system. In The Rat Nervous System. Edited by Paxinos G, London, UK: Academic Press; 1995:923-964.

19. Leinders-Zufall T, Lane AP, Puche AC, Ma W, Novotny MV, Shipley MT, *et al*. Ultrasensitive pheromone detection by mammalian vomeronasal neurons. Nature 2000; 405:792-796.

20. Vickers NJ, Christensen TA, Baker TC, Hildebrand JG. Odour-plume dynamics influence the brain's olfactory code. Nature 2001; 410:466-470.

21. Riffell JA, Shlizerman E, Sanders E, Abrell L, Medina B, Hinterwirth AJ, *et al*. Flower discrimination by pollinators in a dynamic chemical environment. Science 2014; 344:1515-1518.

22. Yamazaki K, Boyse EA, Bard J, Curran M, Kim D, Ross SR, *et al*. Presence of mouse mammary tumor virus specifically alters the body odor of mice. Proc Natl Acad Sci U S A 2002; 99:5612-5615.

23. Kwak J, Willse A, Matsumura K, Curran-Opiekun M, Yi W, Preti G, *et al*. Genetically-based olfactory signatures persist despite dietary variation. PLoS One 2008; 3:e3591.

24. Matsumura K, Opiekun M, Oka H, Vachani A, Albelda SM, Yamazaki K, *et al*. Urinary volatile compounds as biomarkers for lung cancer: a proof of principle study using odor signatures in mouse models of lung cancer. PLoS One 2010; 5:e8819.

25. Guth H. 131. Determination of the configuration of wine lactone. Helv Chem Acta 1996; 79:1559-1571.

26. Furudono Y, Sone Y, Takizawa K, Hirono J, Sato T. Relationship between peripheral receptor code and perceived odor quality. Chem Senses 2009; 31:151-159.

27. Kraft P, Mannschreck A. The enantioselectivity of odor sensation: some examples for undergraduate chemical course. J Chem Educ 2010; 87:598-603.

28. Hamana H, Shou-Xin L, Breuils L, Hirono J, Sato T. Heterologous functional expression system for odorant receptors. J Neurosci Meth 2010; 185:213-220.

29. Spors H, Wachowiak M, Cohen LB, Friedrich RW. Temporal dynamics and latency patterns of receptor neuron input to the olfactory bulb. J Neurosci 2006; 26:1247-1259.

30. Zhou Z, Belluscio L. Coding odorant concentration through activation timing between the medial and lateral olfactory bulb. Cell Rep 2012; 2:1143-1150.

31. Stopfer M, Bhagavan S, Smith SB, Laurent G. Impaired odour discrimination on desynchronization of odour-encoding neural assemblies. Nature 1997; 390:70-74.

32. Kawasaki T, Saka T, Mine S, Mizohata E, Inoue T, Matsumura H, *et al*. The N-terminal acidic residue of the cytosolic helix 8 of an odorant receptor is responsible for different response dynamics via G-protein. FEBS Lett 2015; 589:1136-1142.

33. Rasmussen SG, Choi HJ, Rosenbaum DM, Kobilka TS, Thian FS, Edwards PC, *et al*. Crystal structure of the human β_2 adrenergic G-protein-coupled receptor. Nature 2007; 450:383-387.

34. Cherezov V, Rosenbaum DM, Hanson MA, Rasmussen SG, Thian FS, Kobilka TS, *et al*. High-resolution crystal structure of an engineered human β_2-adrenergic G protein-coupled receptor. Science 2007; 318:1258-1265.

35. Choe HW, Kim YJ, Park JH, Morizumi T, Pai EF, Krauss N, *et al*. Crystal structure of metarhodopsin II. Nature 2011; 471:651-655.

36. Rasmussen SG, DeVree BT, Zou Y, Kruse AC, Chung KY, Kobilka TS, *et al*. Crystal structure of the β2 adrenergic receptor-Gs protein complex. Nature 2011; 477:549-555.

37. Kling RC, Lanig H, Clark T Gmeiner P. Active-state models of ternary GPCR complexes: determinants of selective receptor-G-protein coupling. PLoS One 2013; 8:e67244.

38. Bruno A, Costantino G, de Fabritiis G, Pastor M, Selent J. Membrane-sensitive conformational states of helix 8 in the metabotropic Glu2 receptor, a class C GPCR. PLoS One 2012; 7:e42023.

39. Krishna AG, Menon ST, Terry TJ, Sakmar TP. Evidence that helix 8 of rhodopsin acts as a membrane-dependent conformational switch. Biochemistry 2002; 41:8298-8309.

40. Kuwasako K, Kitamura K, Nagata S, Hikosaka T, Kato J. Structure-function analysis of helix 8 of human calcitonin receptor-like receptor within the adrenomedullin 1 receptor. Peptides 2011; 32:144-149.

41. Knepp AM, Periole X, Marrink SJ, Sakmar TP, Huber T. Rhodopsin forms a dimer with cytoplasmic helix 8 contacts in native membranes. Biochemistry 2012; 51:1819-1821.

42. Herrmann R, Heck M, Henklein P, Henklein P, Kleuss C, Hofmann KP, *et al*. Sequence of interactions in receptor-G protein coupling. J Biol Chem 2004; 279:24283-24290.

43. Delos Santos NM, Gardner LA, White SW, Bahouth SW. Characterization of the residues in helix 8 of the human β1-adrenergic receptor that are involved in coupling the receptor to G proteins. J Biol Chem 2006; 281:12896-12907.

44. Palczewski K, Kumasaka T, Hori T, Behnke CA, Motoshima H, Fox BA, *et al*. Crystal structure of rhodopsin: A G protein-coupled receptor. Science 2000; 289:739-745.

45. Fritze O, Filipek S, Kuksa V, Palczewski K, Hofmann KP, Ernst OP. Role of the conserved NPxxY(x)5,6F motif in the rhodopsin ground state and during activation. Proc Natl Acad Sci U S A 2003; 100:2290-2295.

46. Hamamoto A, Horikawa M, Saho T, Saito Y. Mutation of Phe318 within the NPxxY(x)(5,6)F motif in melanin-concentrating hormone receptor 1 results in an efficient signaling activity. Front Endocrinol 2012; 3:147.

47. Tetsuka M, Saito Y, Imai K, Doi H, Maruyama K. The basic residues in the membrane-proximal C-terminal tail of the rat melanin-concentrating hormone receptor 1 are required for receptor function. Endocrinology 2004; 145:3712-3723.